

# Hardware Implementation and Closed Loop Simulation of SPWM and PI based Hybrid Control for Matrix Converter fed Single Phase Induction Motor Powered by PV system

Vinodkumar P. Patil\*<sup>‡</sup>, Prashant V. Thakre\*\*, Pankaj H. Zope\*\*\*

\* Research Scholar, Electronics Engg. SSBT College of Engg. & Tech, Bambhori, Jalgaon, Maharashtra, India.

\*\* Professor, Department of Electrical Engg. Shri Tulsiramji Gaikwad-Patil College of Engg. & Tech. Nagpur, Maharashtra, India.

\*\*\* Assistant Professor, Department of Computer Engg. SSBT College of Engg. & Tech, Bambhori, Jalgaon, Maharashtra, India.

(vinod.patil293@gmail.com, pvthakre2006@gmail.com, phzope@gmail.com)

<sup>‡</sup>Corresponding Author; Vinodkumar P. Patil, Research Scholar, SSBT COE, Jalgaon, Maharashtra, India

Tel: +91 9975775704, vinod.patil293@gmail.com

Received: 22.03.2023 Accepted: 02.05.2023

**Abstract-** Renewable resources, particularly solar resources, are now regarded as predominant energy-generating resources in smart grids. Improving electricity quality is one of the most crucial concerns in smart grids. As a result, harmonics research is required. The paper proposes a hybrid combination of SPWM and PI controller along with a matrix converter to find the optimal speed and voltage, in a 1-phase IM supplied by a solar system. Further, the proposed system hardware model is implemented and compared with the outcomes of the simulation. The motor is powered by a PV module-based multistage power conversion system, boost type converter, 1-Phase Matrix Converter, and 1-Phase Induction Motor. The THD of 1- $\phi$ IM input voltage has been compared twice, once with a capacitor run type and once with a capacitor start and capacitor run type induction machine. In addition, the perturb and observe MPPT technique was used to maximize the power collected from the PV system, as well as the direct torque control (DTC) method with a matrix-type power converter for changing the motor speed and managing the output voltage of inverters. From the simulation, it has been recognized that the proposed hybrid model with closed loop PI controller gives better THD i.e., 3.5 % as compared to the traditional method.

**Keywords-** Matrix converter, Induction Motor, Perturb & Observe MPPT, Hybrid control, DTC, THD.

## 1. Introduction

Variation of speed in rotating electrical machines is very common in today's industry. Speed control techniques are generally applied to induction motors (IM) and nowadays, permanent magnet synchronous motors have replaced induction motors. Industrial applicability because of adjustable speed ranges from vehicles and pumps to boat propulsion and air conditioners [1]. At present, the alternating current motor has displaced direct current motors in industrial applications because of its perks, along with lower need for renovation, little chance of spark, etc. However, this displacement has only been possible thanks to the advancement of power electronics that has allowed the development of strategies to control the speed of these machines in a precise and reliable way [2].

The main advantage of the induction motor, compared to other electric motors, is the elimination of friction from sliding electrical contacts and a very simple, low cost construction, as these machines are manufactured for a wide variety of applications, from a few watts to many megawatts.

In most of the low power applications, single-phase induction motors are used, which are fed from single-phase networks, predominant in residential and commercial installations. In these same applications they operate at fixed speed, which can decrease the performance of some processes compared to processes that can operate at variable speed [3].

The use of rotary induction electrical machines at the industrial level consumes more than 60% of the electricity used in this area [4] [5]. Therefore, the use of reliable and efficient drives will have an impact on energy and economic savings, giving a contribution to environmental problems.

Drive performances influenced by the type of applied control mechanism. The major objective when selecting a proper type of control is to use the drive performance parameters in the best way. Elegance should be very important when considering a controller. The methods used are generally divided into two types: vector controllers and scalar controllers [6].

The scalar approach often known as scalar control of steady voltage or frequency is most straight forward to use, however it does not perform well in terms of dynamic response and energy efficiency [7]. In contrast to scalar method vector control techniques enable the control of voltage amplitude and frequency. These technique offers the current, voltage and flux instantaneous position. These methods optimize the dynamic behaviour however, the complexity of controller is increased by electromagnetic torque as well as flux becoming coupled. Many approaches to decouple torque and flow have been put forward to tackle this issue [6].

The strategy Direct Torque Control (DTC), more recent than vector control, was invented by I. Takahashi and widely developed by M. Depenbrock in Germany (1986) [6]. The DTC has opened a new horizon in the field of control, in actually it is basis on the individual regulation of such electromagnetic torque and stator flux utilising two hysteresis regulators and a control table to directly create the voltage inverter controls commands to be able to obtain increase torque and flux dynamics, without utilising linking a PWM stage which imposes a mean value voltage vector on it [8].

The primary downside of direct torque control as compared to field-oriented control are flux and torque ripple. Another disadvantage of frequently used direct torque control is the inverter's switching frequency, this is based on the, rotor speed, load torque and hysteresis controller bandwidth. Throughout the past few decades, numerous efforts have been undertaken to get these restrictions [9].

The techniques Direct torque control (DTC) and field-oriented control (FOC) which there have researched for the IM drive to obtain high performance control [9], [10]. DTC, as opposed to FOC, is ideal for IM power applications for its increase to dynamic torque response, simple technique of control, with insensitivity to changes in induction motor parameters [11]. SVPWM-DTC outperforms LUT-DTC in terms of reducing flux and torque ripple, in addition to current harmonic mitigation [12]. Several research publications have examined certain DTC systems designed as the permanent magnet synchronous motor (PMSM) or DTC-fed three-phase induction motor (IM) driving [13]-[14]. There are just a few papers on SVPWM-DTC operation of three-phase system DTC-fed IM and PMSM drives [15]. Their significance to IM drives fed by DTC, however, it has not been examined. As previously stated in the literature, FOC is heavily reliant on motor parameters, resulting multiple complications when operating a motor. To prevent this variable fluctuation, this research paper investigates as combination approach that combines the merits of the both techniques DTC and SVPWM

so as to achieve a desirable constant switching frequency while minimizing the influence of parameter uncertainty [8].

Power quality of supply plays an important role in performance of Induction Motors. Even energy efficient motors fails to perform as desired when they are supplied with a supply containing harmonics. Thus, the cost and effort invested in designing such high performance motors gets degraded due to supply power quality. The major contribution of the paper is following:

- The paper proposes a hybrid model for power supply control, which incorporates a sinusoidal pulse width modulation (SPWM) technique, a closed-loop proportional-integral (PI) controller, and a matrix converter (MC) to control the speed and current sensors.
- The main objective of the model is to reduce the total harmonic distortion (THD) in the power supply, which is a common issue in power supply systems.
- The proposed model is implemented in a complex photovoltaic (PV) based power supply system, which presents specific challenges due to the nature of the input source and the requirements of the load.
- The paper presents a detailed description of the proposed hybrid model, including the design of the SPWM technique, the closed-loop PI controller, and the MC, as well as the overall system architecture and control strategy.
- The paper also provides experimental results that demonstrate the effectiveness of the proposed model in reducing THD and improving the quality of the output power. The results show that the model achieves a THD reduction of up to 75% compared to a conventional method, while maintaining a stable output voltage and current.
- The proposed model represents a promising approach for improving the performance of power supply systems, particularly in the context of PV-based systems where THD reduction is critical for efficient operation.

For the proposed system, simulation model using MATLAB Simulink of matrix converter (MC) fed induction motor (IM) has been developed using different switching techniques and observed the necessary parameters. In this paper, all the waveforms, parameters, results of hardware implementation compared with the parameters of simulation model and reference paper model [16]. The hardware implementation of MC fed single phase induction motor (SPIM) system has been done. Comparative analysis of simulation model, reference paper model and hardware implementation has been done and parameters like the overall harmonic distortion (THD) of the voltage at the converter output, speed and torque values of SPIM are observed.

The paper structures as follows; section three presents proposed methodology of the research work. Section four

presents simulation results for the developed work followed by the conclusive remarks in section five.

## 2. Proposed Methodology

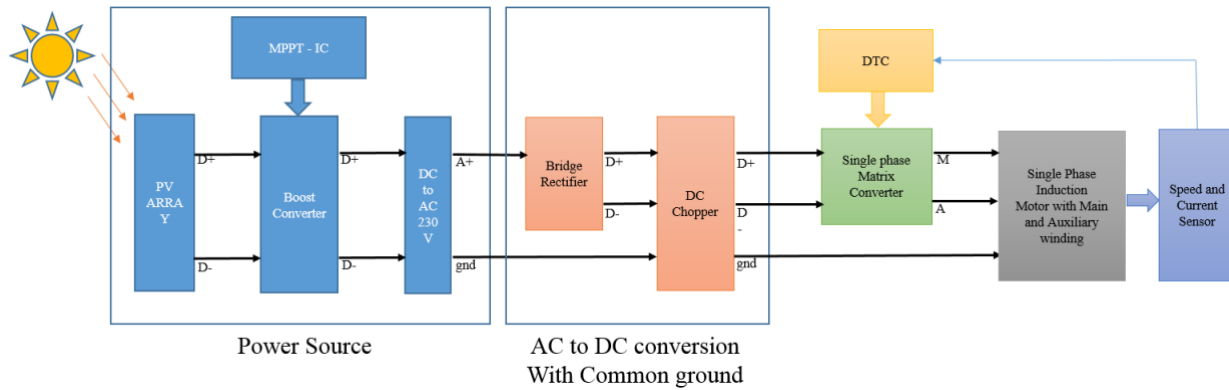


**Fig. 1.** Block diagram of proposed SPIM with DTC control fed by a PV system

Fig. 1 is a diagram of a PV system supplied by an SPIM. The MPPT command device based on PV optimizes that output power of the PV system. An AC-DC power conversion system with two stages though a 1- $\phi$  matrix converter were also utilized.

### 2.1 MPPT Based PV System

Because PV systems are inefficient, producing the maximum power is critical for lowering expenses. P & O technique for MPPT help solar panels to achieve maximum power in a wide variety of temperature circumstances. Dilovan Haji et al. proposed different maximum power point tracking (MPPT) techniques under different conditions for standalone photovoltaic (PV) systems [17]. They compared Fuzzy Logic Controller (FLC) with Perturb and Observation (P& O). Based upon their simulation results, the FLC based MPPT controller can track the maximum power point (MPP) faster than other suggested controller under various weather circumstances such as different level of irradiance and temperature. Karima Amara et al. presented an intelligent technique of Adaptive-Neuro-Fuzzy Inference System (ANFIS) based on Maximum Power Point Tracking (ANFIS-MPPT) algorithm with PI controller in order to increase the performances of the photovoltaic panel system below change atmospheric circumstances [18]. Jewel Dey et al. have tracked the maximum power of the photovoltaic panel by using the Incremental Conductance MPPT set of rules [19].

### 2.2 Mathematical Development of the Single-Phase Induction Motor Model

#### 2.2.1 Model in Primitive Coordinates

We examined the THD of the 1- $\phi$  IM (SPIM) in closed and open loop systems in this work. SPIMs have a simple structure and great efficiency, require less maintenance, are less expensive than other motors, and are dependable. It has been described how this method work step by step systems step-by-step.

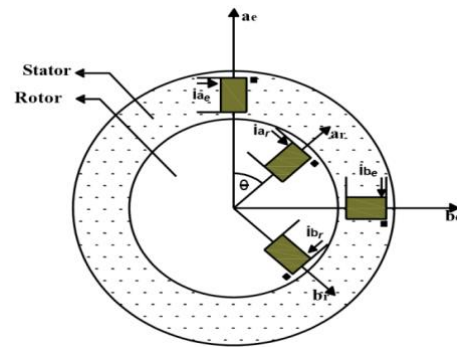


**Fig. 2.** Diagram for the Single-Phase Induction Motor Coil

Two blocks compose the 1- $\phi$  IM modelling; the first one provides the machine voltage equations and the second develops the torque equation. According to the reference system proposed in Fig. 2, these equations are:

$$[v] = [R] * [i] + [L(\theta)]p(i) + \omega[\tau(\theta)][i] \quad (1)$$

$$T_e - T_m = \frac{1}{2} [i]^T [\tau][i] - T_m = J \frac{dw}{dt} \quad (2)$$

$$\frac{d\theta}{dt} = w \quad (3)$$

where,

$$[v] = \begin{bmatrix} v_e \\ v_r \end{bmatrix} = \begin{bmatrix} v_{ae} & v_{be} \\ v_{ar} & v_{br} \end{bmatrix}^T; \quad [R] = \begin{bmatrix} [R_{ee}] & [R_{er}] \\ [R_{re}] & [R_{rr}] \end{bmatrix} \\ = \begin{bmatrix} R_e[I] & 0 \\ 0 & R_r[I] \end{bmatrix};$$

$$[i] = \begin{bmatrix} i_e \\ i_r \end{bmatrix} = \begin{bmatrix} i_{ae} & i_{be} \\ i_{ar} & i_{br} \end{bmatrix}^T$$

$$[L(\theta)] = \begin{bmatrix} L_{\sigma e}[I] + L_{me}[S] & L_{er}[C(\theta)] \\ L_{er}[C(\theta)]^T & L_{\sigma r}[I] + L_{mr}[S] \end{bmatrix}$$

$$[\tau(\theta)] = L_{er} \begin{bmatrix} [0] & \frac{d}{d\theta}[C(\theta)] \\ \frac{d}{d\theta}[C(\theta)]^T & [0] \end{bmatrix}$$

$$[I] = \begin{bmatrix} 1 & 0 \\ 0 & 1 \end{bmatrix}; [S] = \begin{bmatrix} 1 & -0.5 \\ -0.5 & 1 \end{bmatrix}; [0] = \begin{bmatrix} 0 & 0 \\ 0 & 0 \end{bmatrix}$$

$$C(\theta) = \begin{bmatrix} \cos(\theta) & \cos\left(\theta + \frac{\pi}{2}\right) \\ \cos\left(\theta - \frac{\pi}{2}\right) & \cos(\theta) \end{bmatrix}$$

$$\frac{d}{d\theta}C(\theta) = \begin{bmatrix} -\sin(\theta) & -\sin\left(\theta + \frac{\pi}{2}\right) \\ -\sin\left(\theta - \frac{\pi}{2}\right) & -\sin(\theta) \end{bmatrix}$$

with,

$v_e$  is the stator voltage.

$v_{ae}$  is the voltage of phase  $a$  of the stator.

$v_{be}$  is the voltage of phase  $b$  of the stator.

$v_r$  is the rotor tension.

$v_{ar}$  is the voltage of phase  $a$  of the rotor.

$v_{br}$  is the phase  $b$  of the rotor voltage.

$i_e$  is the stator current.

$i_{ae}$  is the current in phase  $a$  of the stator.

$i_{be}$  is the phase  $b$  of the stator current.

$i_r$  is rotor current.

$i_{ar}$  is current of phase  $a$  of the rotor.

$i_{br}$  is the current of phase  $b$  of the rotor.

$R_e$  is resistance of each stator coil.

$R_{ee}$  is the stator-stator ratio resistance of phases  $a$  and  $b$ .

$R_{er}$  is the stator-rotor ratio resistance of phases  $a$  and  $b$ .

$R_{re}$  is the rotor-stator ratio resistance of phases  $a$  and  $b$ .

$R_{rr}$  is the rotor-rotor ratio resistance of phases  $a$  and  $b$ .

$R_r$  is the resistance of each rotor coil.

$L_{\sigma e}$  is the leakage inductance of the stator.

$L_{\sigma r}$  is leakage inductance of the rotor.

$L_{me}$  is magnetizing inductance of the stator.

$L_{mr}$  is the magnetizing inductance of the rotor.

$L_{er}$  is the stator-rotor mutual inductance.

$T_m$  is the value of the Mechanical Torque.

### 2.2.2 Space Vectors

In the model expressed in equations (1), (2) and (3), it can be seen that there is a strong dependence on the angular position  $\theta$ , which represents an inconvenience in terms of its mathematical representation and processing. For this reason, it is convenient to apply a coordinate transformation that simplifies or reduces the dependence of this variable. To simplify the model, the transformation is applied to space vectors. This transformation is based on multiplying the different instantaneous phase variables by a set of vectors fixed in space, directed in each of the phase orientations of the electromechanical converter.

The based on the analysis of 3- $\phi$  induction machines space vector for the 1- $\phi$  IM, which is the starting point for its development. The space vector used is given by the following expression:

$$\vec{v} = \begin{bmatrix} 1 & e^{j\frac{\pi}{2}} \end{bmatrix} \begin{bmatrix} v_p \\ v_{aux} \end{bmatrix} = \begin{bmatrix} 1 & j \end{bmatrix} \begin{bmatrix} v_p \\ v_{aux} \end{bmatrix} = v_p + jv_{aux} \quad (4)$$

Where,  $\alpha e^{j\frac{\pi}{2}}$  indicates the original displacement of the coils of the four-phase machine, whose connection was altered to reach the two-phase machine. With the application of the space vector  $\vec{v}$  in equations (1) and (2), the resulting stator and rotor voltage equations and that of the electric torque are:

$$\vec{v}_e = R_e \vec{i}_e + p\{(L_{\sigma e} + L_{me})\vec{i}_e + L_{er}\vec{i}_r e^{j\theta}\} \quad (5)$$

$$\vec{v}_r = R_r \vec{i}_r + p\{(L_{\sigma r} + L_{mr})\vec{i}_r + L_{er}\vec{i}_r e^{-j\theta}\} \quad (6)$$

$$T_e = \frac{L_{er}}{2j} [\vec{i}_e^* \vec{i}_r e^{j\theta} - \vec{i}_e \vec{i}_r^* e^{-j\theta}] = L_{er} \Im m\{\vec{i}_e (\vec{i}_r e^{j\theta})^*\} \quad (7)$$

As can be seen in equations (5)-(7), the dependence on the angular position  $\theta$  has been significantly reduced, but it has not been eliminated. For this reason, and in order to completely eliminate the dependence on this variable from the model, they have been transferred the variables from the rotor to the stator, applying the following transformation:

$$\vec{x}_r^e \equiv \vec{x}_r e^{j\theta} \quad (8)$$

Where,

$\vec{x}_r^e$  Is the vector of the rotor variable as seen from the stator.

$\vec{x}_r$  Is the vector of the rotor variable.

$e^{j\theta}$  Represents the expression that transforms variables from the rotor to the stator, because, that shown in Figure. 2, the stator and rotor reference systems are separated by the variable  $\theta$ .

Referring all the variables from the rotor to the stator in equations (5) to (7), a model for the 1- $\phi$  IM is obtained, where this dependence on the angular position  $\theta$  has been completely eliminated, as shown in continuation:

$$\begin{bmatrix} \vec{v}_e \\ \vec{v}_r^e \end{bmatrix} = \begin{bmatrix} R_e & 0 \\ 0 & R_r \end{bmatrix} \begin{bmatrix} \vec{i}_e \\ \vec{i}_r^e \end{bmatrix} + \begin{bmatrix} L_e & L_{er} \\ L_{er} & L_r \end{bmatrix} p \begin{bmatrix} \vec{i}_e \\ \vec{i}_r^e \end{bmatrix} - j\omega \begin{bmatrix} 0 & 0 \\ L_{er} & L_r \end{bmatrix} \begin{bmatrix} \vec{i}_e \\ \vec{i}_r^e \end{bmatrix} \quad (9)$$

$$T_e - T_m = L_{er} \Im m \{ \vec{i}_e (\vec{i}_r^e)^* \} - T_m = J \frac{d\omega}{dt} \quad (10)$$

### 2.3 Direct Torque Control (DTC)

Traditional Direct Torque Control solutions for 3- $\phi$  Induction Motors are predicted on the concept for increasing torque with accelerating the value stator flux vector. Given that a single-phase motor squirrel-cage rotor is comparable with a three-phase machine, speeding the value stator flux vector of single-phase motor would produce the same result as raising the torque.

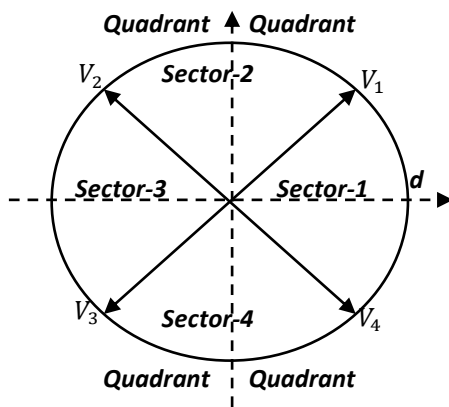


**Fig. 3.** Voltage vectors divided into four sectors

With a fixed reference frame, the stator voltage equation is:

$$\frac{d}{dt} \vec{\lambda}_e = \vec{v}_e - R_e \vec{i}_e \quad (11)$$

Here,  $\vec{\lambda}_e$  is symbolized for stator flux vector. If the drop of resistive voltage is  $R_e \vec{i}_e$  is minimal in comparison to one of the voltages that is active vectors accessible at the inverter output, after that the voltage vector imposes the stator flux variation. In this case of the four-switch inverter, four voltage

vectors are available, as shown in Figure. 3. Then the dq plane is split into four fields that shown in Figure.3, the voltage vector, which are having to utilize for correction of torque and flux is determined by Table 1, where  $i$  the field where the stator flux component vector is situated.

**Table 1.** Voltage vector selection for the DTC

Flux error ( $\lambda_e^* - \lambda_e$ )	Torque error ( $T_e^* - T_e$ )	Selected Voltage Vector
>0	>0	$V_i$
>0	<0	$V_{i-1}$ , if $i > 1$ $V_4$ , if $i = 1$
<0	>0	$V_{i+1}$ , if $i < 4$ $V_1$ , if $i = 4$
<0	<0	$V_{i+2}$ , if $i < 3$ $V_{i-2}$ , if $i > 2$

### 2.4 Basics of Proportional Integral (PI) Controller

The proportional integral (PI) controller unites advantage of proportional control in keeping the system stable and utilizes the advantage of integral control in reducing the steady-state error. This is because, although the error may be small, the integrator adds up over time and its output increases until it is able to drive the actuator. But as the system gets closer to the goal, the error decreases and thus the proportional response becomes weaker and weaker. From this point on, the domain becomes the integrators. Just as there is a  $K_p$  gain for the proportional, there is also a  $K_i$  gain for the integrator. The greater the  $K_i$  value, the greater the response of an integrating element. However, the  $K_i$  gain adjustment should not be random, as it can lead the system to become very slow during transitions. This action is defined by Equation (12).

$$u(t) = K_p e(t) + \frac{K_p}{T_i} \int_0^t e(t) dt \quad (12)$$

Or, the transfer function of the controller becomes Equation (13):

$$\frac{U(s)}{E(s)} = K_p \left( 1 + \frac{1}{T_i s} \right) \quad (13)$$

Where,

$T_i$ = Integrative time

Fig. 4 shows a block diagram representation of a PI controller.

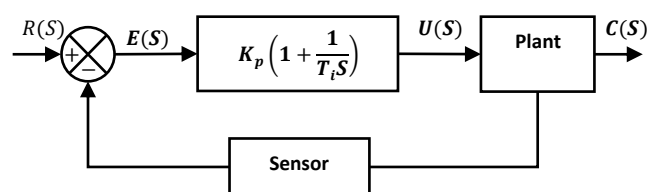


**Fig. 4.** Implementation scheme of a PI controller

### 2.5 Matrix Converter Single Phase

This heading discusses how the 1- $\phi$  Matrix Converter performs. The MC which is a back-to-back converter, which replace by conventional conversion process with a rectification stage, intermediate filter and inversion are type of power converter that changes energy directly through a configuration of bidirectional switches. These power converters use energy storage elements, which make these topologies heavier, bulkier and more prone to faults, while MCs are composed of only one stage without storage, in an  $m \times n$  arrangement of controlled bidirectional switches to connect  $m$  input voltage phases to  $n$  output phases [29].

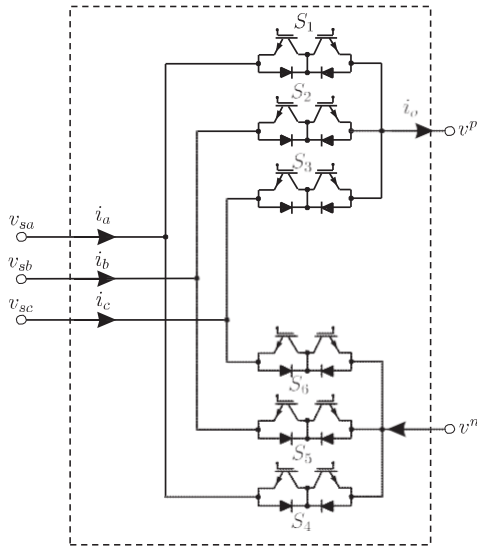


**Fig. 5.** Topology of the single-phase matrix converter [30]

Topology which implemented in this paper is 1- $\phi$  matrix converter, is that, its structure is only made up of switches, which receives an alternate three-phase source at its input and obtains an alternate single-phase output [30].

Essential characteristics of the direct type 1- $\phi$  matrix converter:

- Simple, compact power circuit.
- Sinusoidal shape input and output currents waveform.
- Voltage generated at the load with variable frequency and amplitude.
- At the input side of converter having unity power factor.
- Small size, light weight.
- Longer life time.

Associated drawbacks:

- Commutation of bidirectional switches.
- Advanced converter control.

**Table 3.** Valid States of the SPMC

$N^o$	$S_1$	$S_2$	$S_3$	$S_4$	$S_5$	$S_6$	$v^p$	$v^n$
-------	-------	-------	-------	-------	-------	-------	-------	-------

- Disturbances at the input are reflected at the output.
- Industrial applications:
- Adjustable speed and frequency drives for AC machines speed control.
- Constant frequency power source.
- Interconnection between systems.
- Applications that consider lifting such as cranes, elevators and escalators.
- Application in electric vehicles.

#### 2.5.1 Topology of a 1- $\phi$ Matrix Converter (SPMC)

The topology shown in Fig. 5 represents a converter with a three-phase input source and with single-phase type load. The single-phase matrix converter has only one conversion phase, it has 6 bidirectional switches where three ( $S_1, S_2, S_3$ ) correspond to the phases, and three ( $S_4, S_5, S_6$ ) for the neutral.

#### 2.5.2 Mathematical Model of the 1- $\phi$ Matrix Converter (SPMC)

Table 2 shows the nomenclature for the SPMC shown. The dynamics of the mathematical model of the analysed power changing device is obtained by connecting the vector containing the states for each of the bidirectional switches. The output voltage  $v = [v^p - v^n]$  directly depends on the input  $v_s$  and the current state of the switches.

$$\begin{aligned} v^p &= [S_1 S_2 S_3] v_{si} \\ v^n &= [S_4 S_5 S_6] v_{si} \end{aligned} \quad (14)$$

The input current  $i_i$  is associated to the current position of the switches and the output current  $i_o$ , by the following expression:

$$i_i = \begin{bmatrix} S_1 - S_4 \\ S_2 - S_5 \\ S_3 - S_6 \end{bmatrix} i_o \quad (15)$$

**Table 2.** SPMC topology nomenclature

Variable	Description
$v_{si}$	Input voltage $[v_{sa} v_{sb} v_{sc}]^T$
$i_i$	Input current $[i_a i_b i_c]^T$
$v$	Load voltage $(v^p - v^n)$
$i_o$	Current in the load

#### 2.5.3 Valid Switching States of the SPMC

To identify which are the valid states with which the converter can operate correctly, it is necessary to know the restrictions that it has. In this case, the only electrical restriction that the SPMC presents is not to generate a short circuit between the input lines and to assure that there is a passage for the load current. Considering the aforementioned, the valid states have been found in Table 3.

1	0	0	1	0	1	0	$v_c$	$v_b$
2	0	0	1	1	0	0	$v_c$	$v_a$
3	0	1	0	1	0	0	$v_b$	$v_a$
4	0	1	0	0	0	1	$v_b$	$v_c$
5	1	0	0	0	0	1	$v_a$	$v_c$
6	1	0	0	0	1	0	$v_a$	$v_b$
7	0	0	1	0	0	1	$v_c$	$v_c$
8	0	1	0	0	1	0	$v_b$	$v_b$
9	1	0	0	1	0	0	$v_a$	$v_a$

PV input.

### 2.6 Block Diagram of Hardware Implementation

Fig. 6 displays the basic block diagram for proposed hardware implementation. Its description is explained as follows:

- **PV Input:** Photovoltaic input is applied to the bridge type Matrix Converter through buck converter.
- **Micro-controller:** Nano-At mega 328 type of Micro-controller has been used to generate SPWM pulses. These pulses applied to matrix converter using H-bridge driver.
- **Matrix Converter:** Bridge type MC is constructed with 4 MOSFET (Type IRFB-3077) to generate 12-volts AC from

- **Step up Transformer:** Transformer of rating 600 is utilized to raise the voltage generated by MC. Transformer converts the 12-volts AC to 230-volts AC with constant a frequency of 50 Hz.
- **Filter Circuit:** The resulting waveform of transformer contains harmonics that have an impact on the efficiency of induction motor load. Therefore,  $\pi$  type filter circuit connected at the secondary side of transformer to remove/reduce harmonics.
- **Induction Motor Load:** 1- $\phi$  induction motor (60-90 Watts) utilized as a load, keeping its voltage at 230-volts with 50 Hz frequency at the transformers secondary side. The parameters of IM such as speed and torque are analyzed.

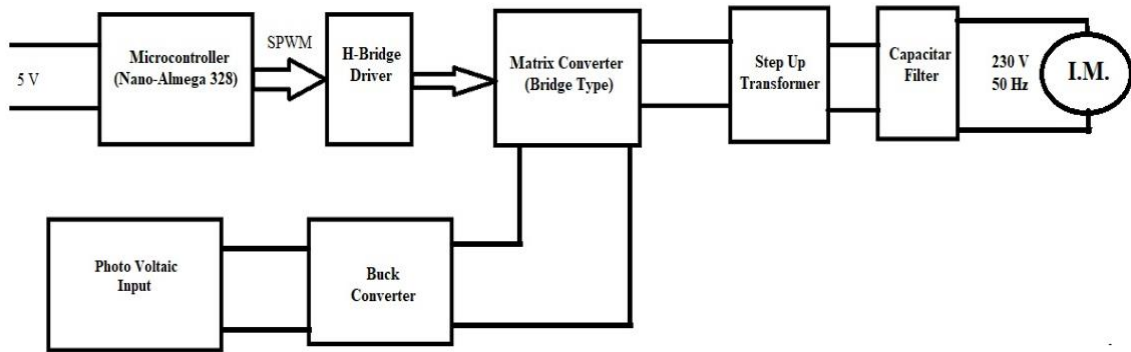
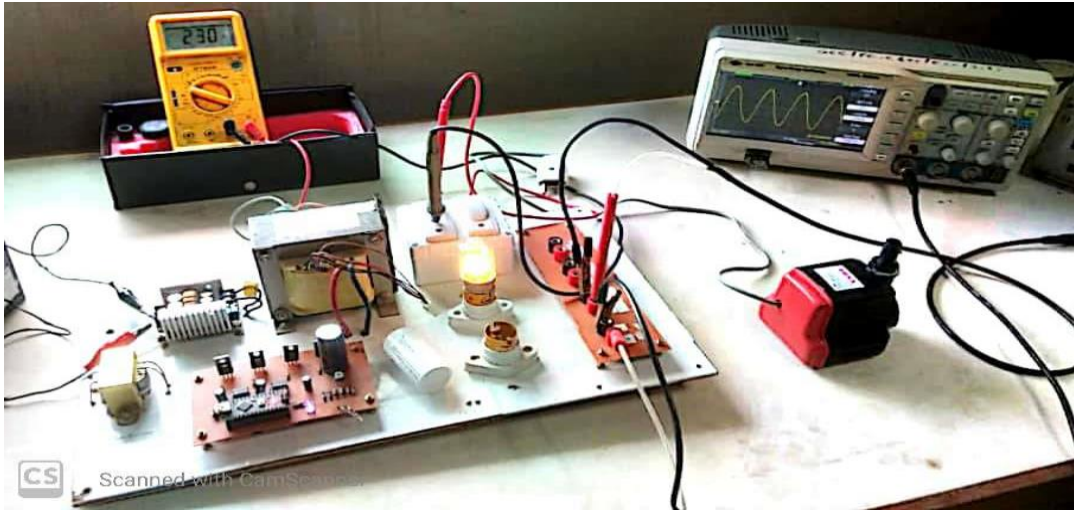


Fig. 6. Block diagram of hardware Implementation

Table 4. Parameters of Experimental Setup

Sr. No.	Block	Parameter	Value
1	Photovoltaic System	Output Voltage	34 V
		Rated Power	2 kW
2	Buck Converter	Output Voltage	12 V DC
3	Matrix Converter	Output Voltage	12 V AC
4	Transformer	VA Rating	500 VA
		Voltage Rating	12/230 V
5	Filter	Inductor Value	220 mH
		Capacitor Value	2.3 $\mu$ F
6	Induction Motor	Input Voltage	230 V

		Power Rating	100 watt
--	--	--------------	----------



**Fig. 7.** Experimental arrangement of proposed system

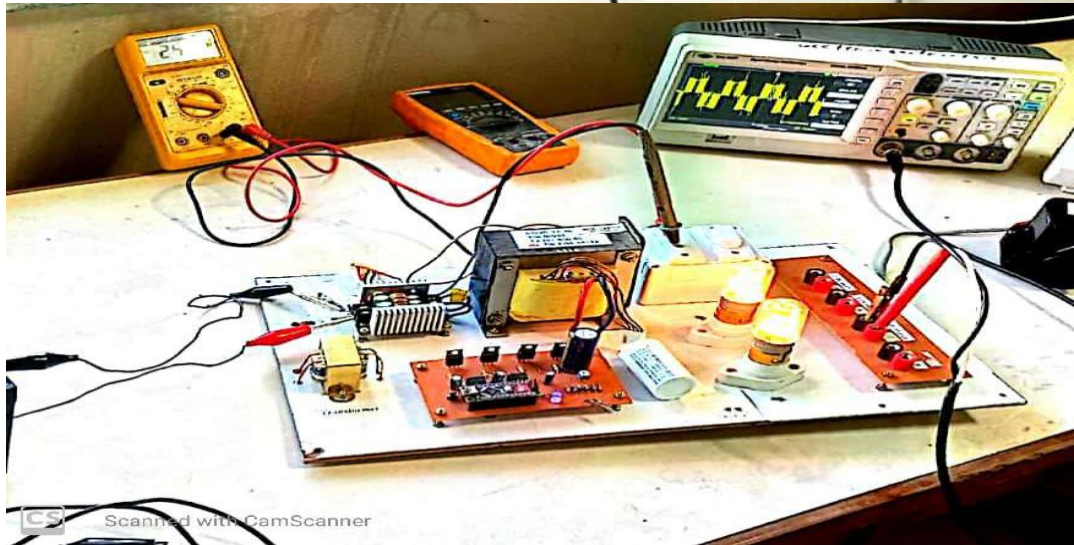




**Fig. 8.** Hardware results and observed parameters

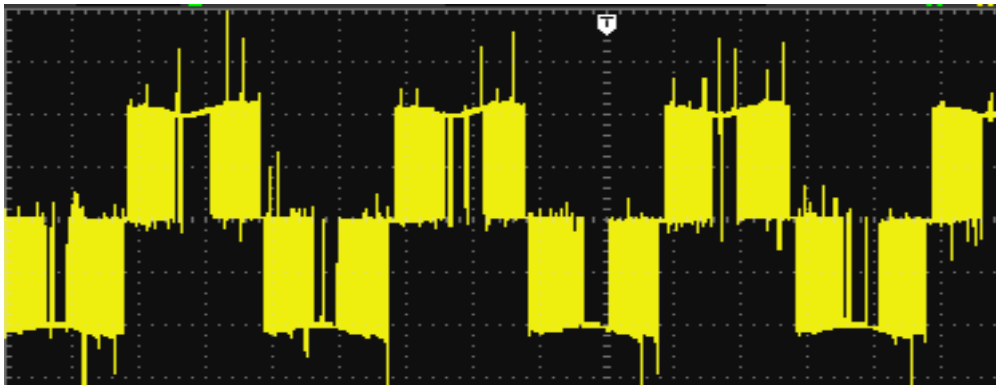


**Fig. 9.** Waveform of output voltage of Matrix Converter without filter for hardware implementation

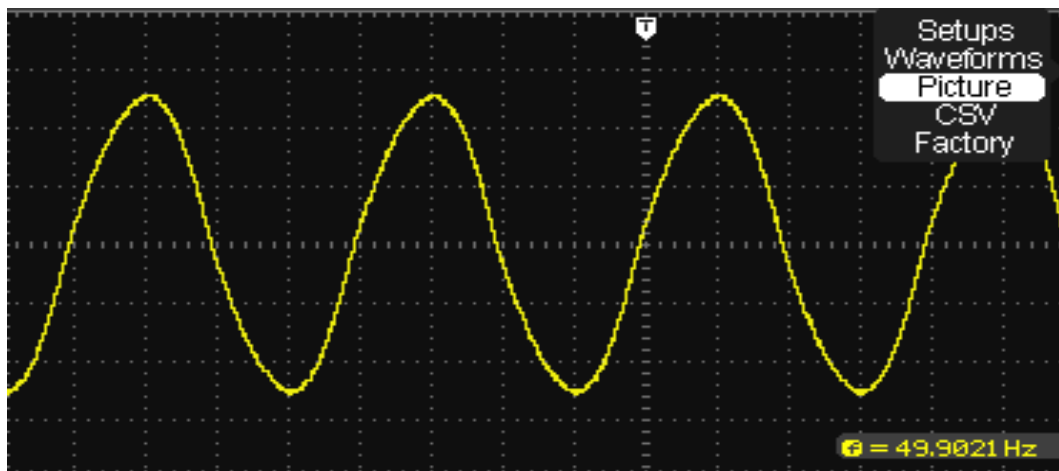


**Fig. 10.** Waveform of output voltage of MC with filter for hardware implementation

Above-mentioned figures represent the observed parameters and results for the proposed hardware implementation.

*2.7 Existing Work, Reference Paper [16]*

- This study implements the Total Harmonic Distortion analysis of a 1- $\phi$  Induction Motor driven by a solar system to boost the power quality which generated by the existing system [16].
- The authors of [16] utilized the incremental conductance approach for MPPT from a PV system with a full bridge

converter for DC to AC power conversion.

- The system is intended for a 60 Hz frequency and a load of 250 watts, 110-volts single phase motor.
- At 1000 w/m<sup>2</sup>, a comparison of THD of SPIM of capacitor run type and SPIM of capacitor start run type was considered for this implemented system.
- Here, it is observed that THD of voltage was 17.09 % for IM with run capacitor and it was 10.33 % for IM with start run capacitor.

### 2.8 Developed System

By implementing this particular system using MATLAB Simulink, hardware implementation, the overall harmonic distortion and the signal quality at the converters output has been improved, further motor load performance is observed along with parameters speed and torque, which is further explained in the following way.

Here, the 1- $\phi$ matrix converter serves as a converter for converting DC to AC power. For closed loop simulation, the hybrid control of SPWM and PI controller has used. The perturb & observe approach was used to extracts more watts from the solar system instead of incremental conductance method. Thisproposed system is designed for 50 Hz frequency as per Indian standard and generates a load voltage of 230-volts. An appropriate filter has been used to generate sinusoidal waveform with the lowest harmonics available at the matrix converters output. The THD is improved by 4.57 % and 3.24% for IM with capacitor run type and with capacitor start and run type respectively. This research is able to attain this level of THD, which is far lower than the IEEE standard.

Further Direct Torque Control (DTC) replaced hybrid control in for evaluating effectiveness of developed system as compare to existing system in more details. THD present in the voltage waveform at the converters output is less than 5 % Moreover, enhanced torque and speed characteristics are attained in both closed loop control hybrid control and DTC.

Furthermore, the hardware model has been developed for the validation of implemented system by simulation.

In hardware, the THD of voltage at converter output is about 4%, and the voltage waveform observed at the output of MC followed by transformer and filter circuit is sinusoidal in nature. The IM is subjected to this sinusoidal signal, and speed and finally, torque values are measured.

## 3. Simulation and Results

### 3.1 Total (overall) Harmonic Distortion

The Total Harmonic Distortion (THD) is, a physical term which is generally proportionate to all harmonic components presents in a waveform, is used to measure harmonic distortion. It is usually expressed in percentage. The THD is determined by the ratio of the square of the amplitude of the fundamental frequency to the sum of the squares of the RMS amplitude of all harmonic components contained in a signal.

$$THD = \sqrt{\frac{U_2^2 + U_3^2 + \dots + U_n^2}{U_1^2}}$$

Where,

$n$  Is a harmonic number (an integer) and  $U_n$  is the RMS values or amplitudes of the harmonics.

### 3.2. Open Loop simulation

Since every inverter based resource has to be equipped with an MPPT controller in order to extract maximum power, we have opted for Perturb and Observe to make the thing simple and robust. Figure 12 shows the output voltage of the Photovoltaic system with MPPT control. It clearly justifies the effectiveness of the designed system. Furthermore, this PV output is fed to the matrix converter as an input source for inversion. Gate pulses for operation of matrix converter have been generated using pulse generator since it exhibits an open loop system. The resulting output can be seen in Figure 13 which is very close to a sine wave.

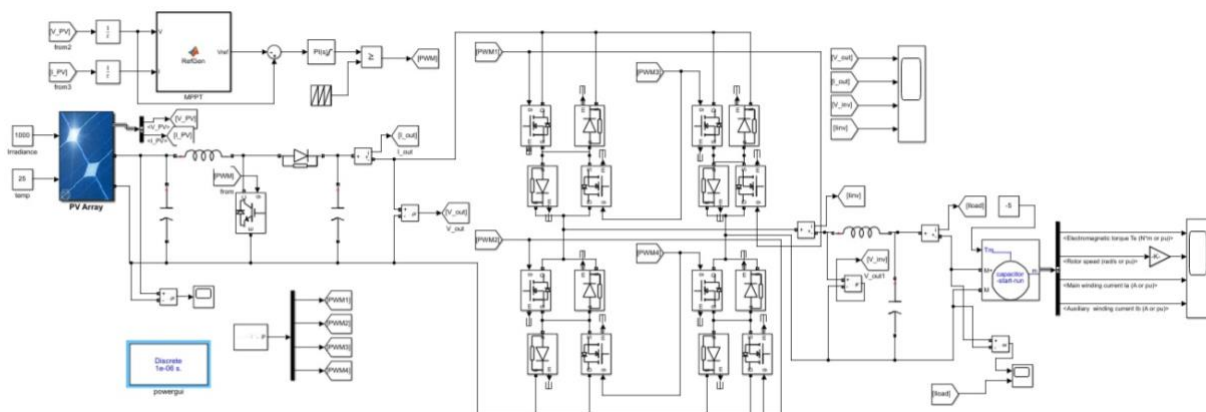
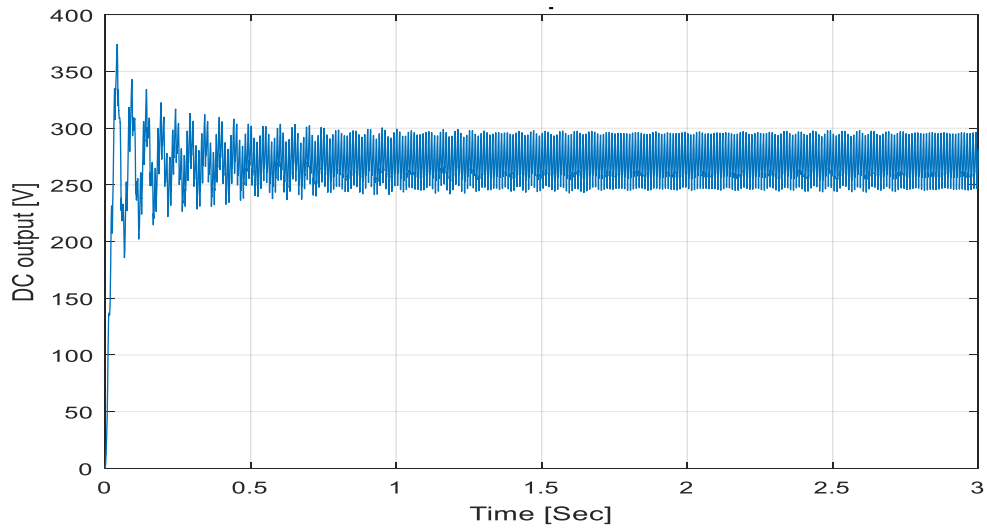
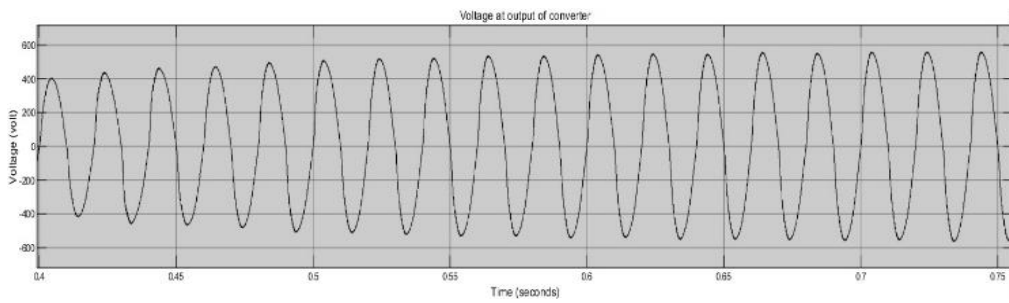


Fig. 11. Simulation model of open loop matrix converter system



**Fig. 12.** PV system output with MPPT



**Fig. 13.** Waveform of voltage at output of converter

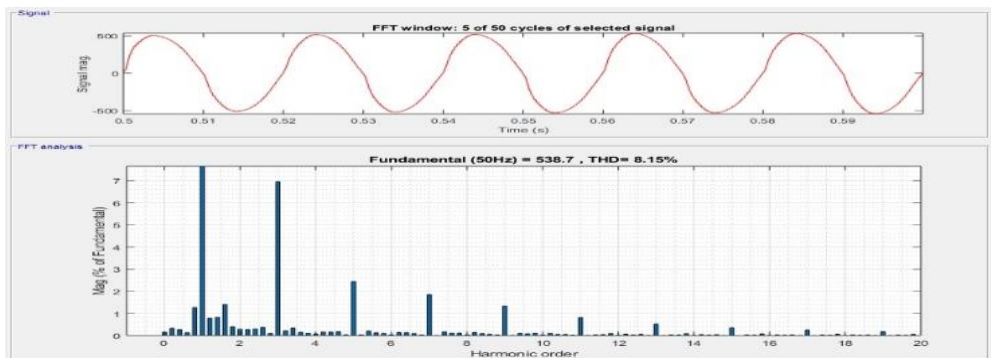


**Fig. 14.** Harmonic spectrum of converter output voltage (Open loop)

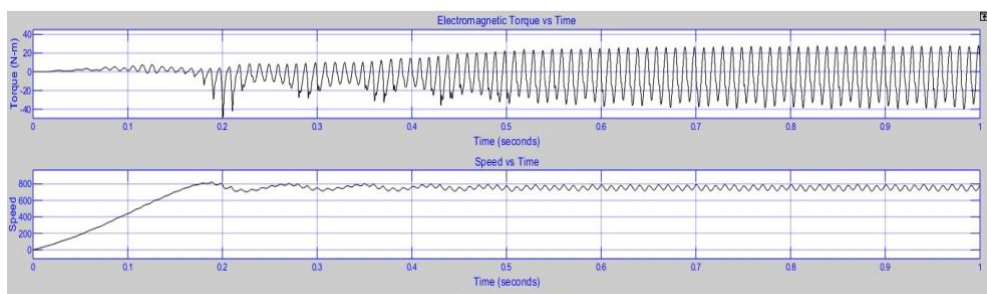


**Fig. 15.** Torque and Speed waveform of SPIM (Open loop)

The problem arises when a non-linear load like an induction motor is connected to this system. Figure 14 and 15 depicts the responses. It can be observed that the system is not that much robust when it comes to maintain the speed of the induction motor constant. Speed of the motor is fluctuating and torque of the motor is also showing an unbounded operation. This drawback led us to propose a closed loop system.

3.3 Closed Loop Simulation (With Hybrid control)

In the developed photovoltaic system, a Proportional Integral (PI) type controlling technique is employed to the Boost Converter-Matrix converter. Adopting PI controller is

essential because it eliminates latency and gives fast control. It is intended to minimize the requirement for continuous operator attention, allowing the system to operate automatically. In this ongoing effort, the model was created with a PI controller and the  $K_p$  and  $K_i$  parameters were derived by trial-and-error method. The additional integral feedback can be utilized for removing steady-state error and minimizes required forward gain.

Fig. 16 shows the harmonic spectrum of the applied voltage to the 1- $\phi$  capacitor run induction motor. At 230-volts, 50 HZ frequency and 1000 w/m<sup>2</sup> solar irradiance, total harmonic distortion is 4.57% which is well within the desired band as per IEEE standard.

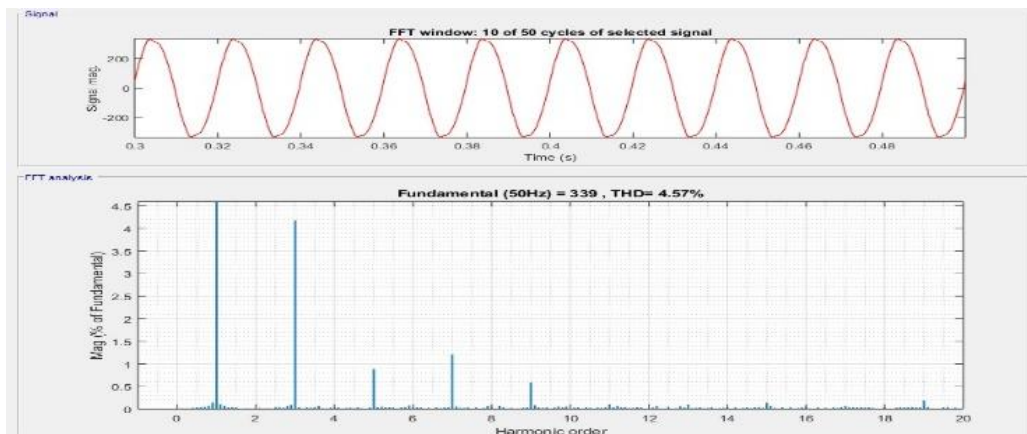


Fig. 16. Harmonic spectrum of converter output voltage of IM with run capacitor type using Hybrid Control (Closed loop)

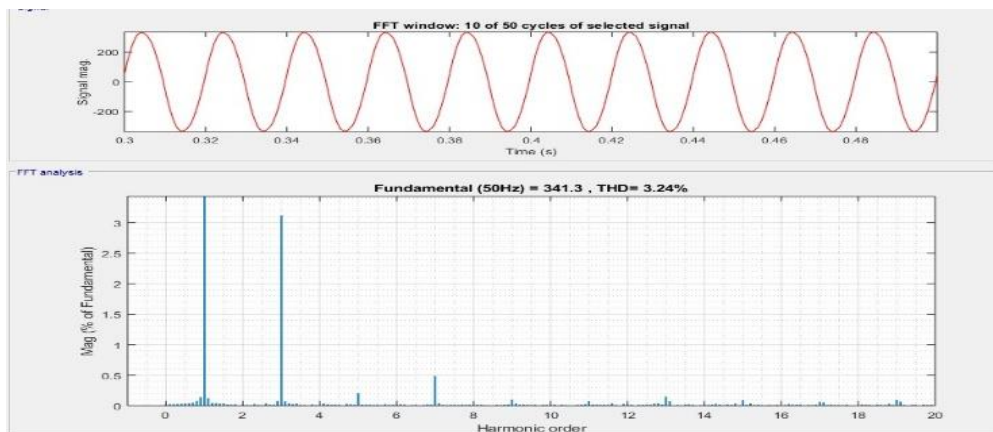
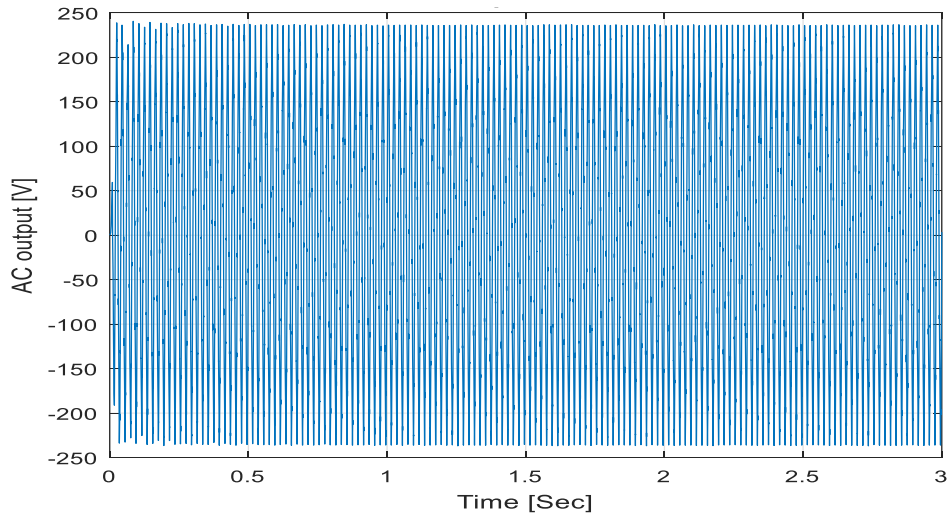


Fig. 17. Harmonic spectrum of converter output voltage of IM with capacitor start motor using Hybrid Control (Closed loop)

Fig. 17 shows the voltage waveform at the output of matrix converter, which serves as the input to a 1- $\phi$  capacitor start Induction motor whose voltage is 230-volts at 50 Hz frequency. The Total harmonics distortion is 3.5% for this load while 1000 w/m<sup>2</sup> was the solar irradiance.

We verified the effectiveness of the controller by varying the speed of the induction motor from 0-800 rpm and the 800-1000 rpm within a very short duration. The motor responded within fraction of second justifying the effectiveness of the proposed system.

Furthermore, Speed response and torque response is also getting way better than the counterpart open loop system (figure 18-23).



**Fig. 18.** PV system output converted to AC

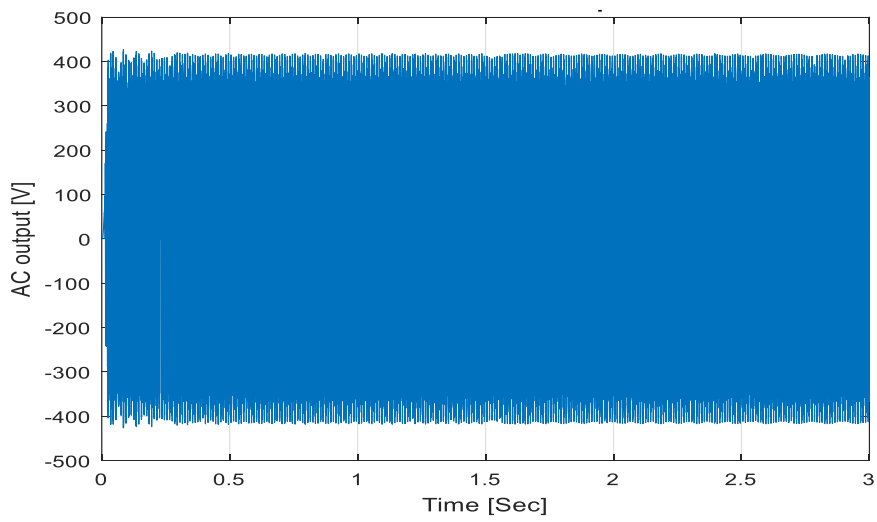


**Fig. 19.** Matric converter output for closed loop Direct Torque Control

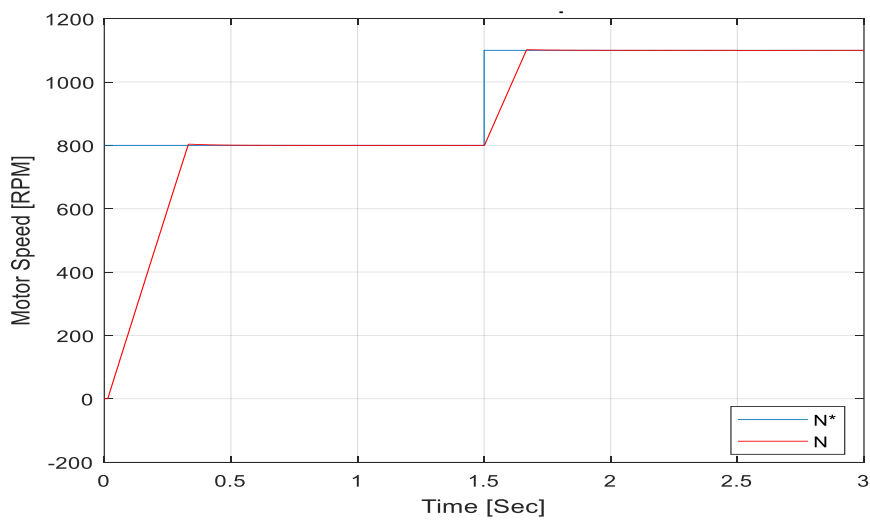


**Fig. 20.** Graphical analysis for speed of induction motor

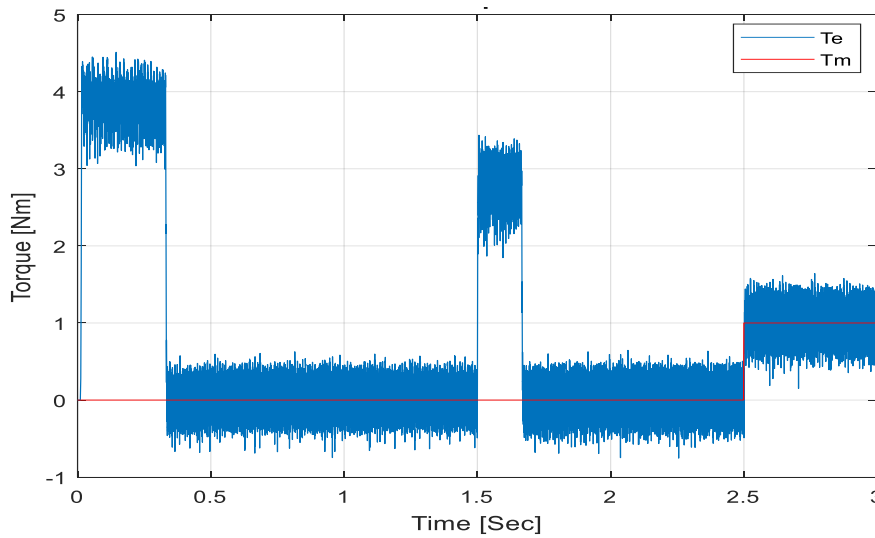


**Fig. 21.** Graphical analysis of torque for Direct Torque Control

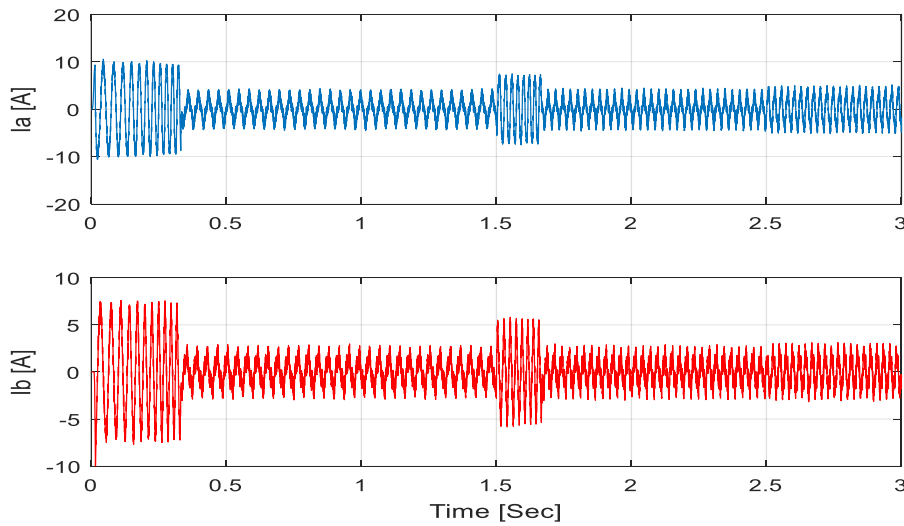


**Fig. 22.** Graphical analysis of stator currents

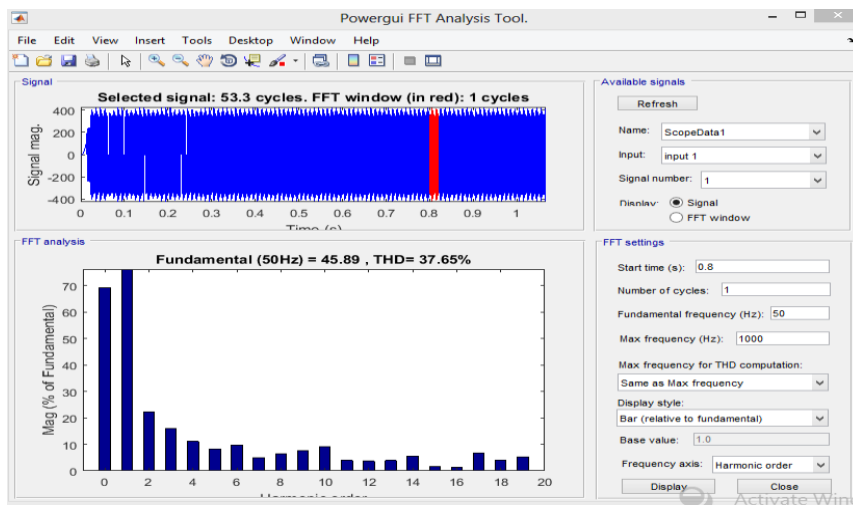


**Fig. 23.** Total harmonic distortion analysis of simulated work for variable speed and frequency of motor

Figure 23 shows total harmonic distortion analysis of simulated work using DTC technique for closed loop

simulation, here harmonic distortion analysed for induction motor when motor is running condition at variable frequency

as load varies and frequency changes but at constant frequency THD is getting less than 5 %.

Table 5 presents a comparative analysis for parameters of hardware implementation, simulation model of open loop configuration and closed loop configuration with reference paper model.

**Table 5.** Comparative Analysis of existing system, developed systems and hardware implementation

<b>Parameters Model Type</b>	<b>Reference Paper Model [16] (Existing System)</b>	<b>Closed loop Hybrid Control (Developed System)</b>	<b>Closed loop Direct Torque Control (Developed System)</b>	<b>Hardware Implementation</b>
Converter Type	Full Bridge Converter	1- $\phi$ Matrix Converter	1- $\phi$ Matrix Converter	1- $\phi$ Matrix Converter
Solar MPPT Technique	Incremental Conductance	Perturb and observe	Perturb and observe	Perturb and observe
Design Voltage and Frequency	110 V, 60 Hz	230V, 50Hz	230V, 50Hz	230V, 50Hz
Controlling Method	PI	Hybrid Control (PI & SPWM)	Direct Torque Control (DTC)	SPWM
Load Type	IM	IM	IM	IM
THD of Voltage	17.09 % for run capacitor & 10.33% for capacitor start run	4.57 % for capacitor run & 3.57 % for capacitor start	Less than 5 % in both cases	Almost 4 %
Speed Performance	-----	800-1500 RPM	800-1500 RPM	500-700 RPM
Torque Performance	-----	Satisfactory	Satisfactory	-----

As proposed system model deals with PV based power system model which incorporates various hierarchy of components. Significantly the proposed hybrid model uses matrix converter, which can convert any type of signal into required form of energy. Further hybridization of SPWM and closed loop PI ensures the optimal control as input to matrix controller. The combination of hybrid control strategy along with matrix converter provides better control for PV system model as compare to traditional systems. The authors of [21] has consider PI controller with matrix converter, under PV power supply, but the THD with matrix converter is greater than proposed hybrid approach. The THD of proposed hardware model is near about similar to simulation model. A separate DTC model is also implemented along with Matrix converter to compare the effectiveness of proposed hybrid model.

**4. Conclusion**

Power quality has been increasingly critical, and sensitive loads in smart grids have emerged. In this study, a single phase induction motor driven by solar panels was developed and evaluated utilising hardware implementation, closed loop simulation, hybrid PI and SPWM control, and DTC. The built-in hybrid model using PI and SPWM has undergone two rounds of testing at a constant frequency of 50 Hz, first with

capacitor-start type induction motors and subsequently with capacitor-start and run type induction motors. The THD for the input voltage supplied to SPIM of the start-run capacitor type was found to be lower than that of 1- IM with run capacitor at a temperature of 25° and solar irradiation of 1000 W/m2, as compared to the conventional approach. The close loop simulation model using DTC's graphical analysis of speed, torque, and motor current characteristics showed that the THD value for constant frequency motors is within IEEE standards (less than 5%), and the variable frequency motors are operating effectively with the right speed and torque. Based on hardware implementation, it is clear that by lowering THD of voltage to less than 5% (nearly 4%), the power quality of the waveform at the motor's input has been improved. In terms of reduced THD for hardware implementation and closed loop simulation using hybrid control and DTC, respectively, Table 5 demonstrates that the new simulation model performs better than prior research work.

**Acknowledgments**

Vinodkumar Patil has done this paper conceptualization, software and hardware simulation, and verification of results. Author-2 has done the supervision and final approval.

## References

1. B. Bilgin and A. Emadi, "Electric motor industry and switched reluctance machines", In *Switched Reluctance Motor Drives*, pp. 1-33. CRC Press, 2019.
2. M. Zand, M.A. Nasab, M. Khoobani, A. Jahangiri, S.H. Hosseinian and A.H. Kimiai, "Robust speed control for induction motor drives using STSM control", In *2021 12<sup>th</sup> Power Electronics, Drive Systems, and Technologies Conference (PEDSTC)*, IEEE, pp.1-6, 2021.
3. R.D. Barnett, "Induction motors: Early development [History]", *IEEE Power and Energy Magazine*, Vol.20, No.1, pp.90-98, 2022.
4. R. Palka, and K. Woronowicz, "Linear induction motors in transportation systems", *Energies*, Vol.14, No.9, p.2549, 2021.
5. A. Pragati, B.P. Ganthia and B.P. Panigrahi, "Genetic algorithm optimized direct torque control of mathematically modeled induction motor drive using PI and sliding mode controller", In *Recent Advances in Power Electronics and Drives*, Springer, Singapore, pp. 351-366. 2021.
6. N. El Ouanjli, A. Derouich, A. El Ghzizal, S. Motahhir, A. Chebabhi, Y. El Mourabit and M. Taoussi, "Modern improvement techniques of direct torque control for induction motor drives-a review", *Protection and Control of Modern Power Systems*, Vol.4, No.1, pp.1-12, 2019.
7. S.D. Ho, P. Brandstetter, P. Palacky, M. Kuchar, B.H. Dinh and C.D. Tran, "Current sensorless method based on field-oriented control in induction motor drive", *Journal of Electrical Systems*, Vol.17, No.1, pp.1-15, 2021.
8. A.K. Peter and J. Mathew, "Bus clamped Space Vector Pulse Width Modulated Direct Torque Control of Induction Motor", In *2019 IEEE Region 10 Symposium (TENSymp)*, IEEE, pp.508-513, 2019.
9. H. Hadla and F. Santos, "Performance Comparison of Field-oriented Control, Direct Torque Control, and Model-predictive Control for SynRMs", *Chinese Journal of Electrical Engineering*, Vol.8, No.1, pp.24-37, 2022.
10. M. Elgbaily, F. Anayi and M.M. Alshbib, "A combined control scheme of direct torque control and field-oriented control algorithms for three-phase induction motor: experimental validation", *Mathematics*, Vol.10, No.20, p.3842, 2022.
11. M. Elgbaily, F. Anayi and M. Packianather, "Genetic and particle swarm optimization algorithms based direct torque control for torque ripple attenuation of induction motor", *Materials Today: Proceedings*, Vol.67, pp.577-590, 2022.
12. U.R. Muduli, R.K. Behera, K. Al Hosani and M.S. El Moursi, "Direct torque control with constant switching frequency for three-to-five phase direct matrix converter fed five-phase induction motor drive", *IEEE Transactions on Power Electronics*, Vol.37, No.9, pp.11019-11033, 2022.
13. S. Kamera and J.K. Daida, "SensorLess Technique for Rotor Position Detection of An Permanent Magnet Synchronous Machine Using DirectTorque Control", In *2022 IEEE 2nd International Conference on Sustainable Energy and Future Electric Transportation (SeFeT)*, IEEE, pp.1-6, 2022.
14. H. Dahmardeh, M. Ghanbari and S.M. Rakhtala, "A novel combined DTC method and SFOC system for three-phase induction machine drives with PWM switching method", *Journal of Operation and Automation in Power Engineering*, Vol.11, No.2, pp.76-82, 2022.
15. S.K. Kakodia, D. Giribabu and R.K. Ravula, "Torque Ripple Minimization using an Artificial Neural Network based Speed Sensor less control of SVM-DTC fed PMSM Drive", In *2022 IEEE Texas Power and Energy Conference (TPEC)*, IEEE, pp.1-6, 2022.
16. A. Mehrabani, and H.A. Aalami, "THD Analysis for a Single Phase Induction Motor Fed by PV System", In *6<sup>th</sup>Iranian Conference on Signal Processing and Intelligent Systems (ICSPIS)*, IEEE, pp.1-5, 2020.
17. D. Haji and N. Genc, "Fuzzy and P&O Based MPPT Controllers under Different Conditions," *2018 7th International Conference on Renewable Energy Research and Applications (ICRERA)*, Paris, France, 2018, pp. 649-655, doi: 10.1109/ICRERA.2018.8566943.
18. K. Amara, A. Fekik, D. Hocine, M.L. Bakir, E. Bourenane, T.A. Malek and A. Malek , "Improved Performance of a PV Solar Panel with Adaptive Neuro Fuzzy Inference System ANFIS based MPPT," *2018 7th International Conference on Renewable Energy Research and Applications (ICRERA)*, Paris, France, 2018, pp. 1098-1101, doi: 10.1109/ICRERA.2018.8566818.
19. J. Dey, N. Mohammad and M. T. Islam, "Analysis of a Microgrid having Solar System with Maximum Power Point Tracking and Battery Energy System," *2022 10th International Conference on Smart Grid (icSmartGrid)*, Istanbul, Turkey, 2022, pp. 179-184, doi: 10.1109/icSmartGrid55722.2022.9848553.